The design of a flexible RF generator for driving Acousto-Optical devices in space applications

J Vanhamel[1,2,3] and D Stutman[1]

[1] Faculty of Aerospace Engineering, Space Systems Engineering section, TU Delft, Kluyverweg 1, 2629 HS Delft, The Netherlands
[2] Electronic Circuits and Systems, KU Leuven, Kleinhoefstraat 4, 2440 Geel, Belgium
[3] Royal Belgian Institute for Space Aeronomy, Engineering department, 1180 Brussels, Belgium

j.a.m.vanhamel@tudelft.nl

Abstract. Acousto-Optical (AO) devices are not only used for filtering purposes in spectral imaging, but also in optical communications and spatial tracking systems. Some AO devices with space applications are AO Tunable Filters (AOTFs), Modulators (AOMs), Deflectors (AODs) and Frequency Shifters (AOFSs). Though these device's applications differ, they are all controlled with Radio-Frequency (RF) signals. These signals are converted by a transducer into an acoustic wave, which propagates inside the AO device. The interaction between the incoming light and the acoustic waves inside the birefringent AO material creates multiple output beams. This interaction can result in filtering, modulation, deflection or frequency shifting, depending on the AO device in question. This research focuses on the design of a flexible, uniform RF generator, applicable to all AO devices in the space applications domain. The RF output maximizes the performance of the AO device, while the use of components available in space qualified grades eases integration with future space missions. Its design is a key step towards a miniaturized, space qualified, general-purpose RF generator. This research presents schematics, design and preliminary component test results.

1. Introduction

The use of Acousto-Optical (AO) devices in space applications is growing, mainly due to their robustness, flexibility and wide applicability. These devices are used for multiple purposes in scientific research, as well as in commercial setups. Applications include optical communications [1], spatial tracking systems [2] and the filtering of specific optical wavelengths in spectral imaging of scientific space missions [3]. An AO Tunable Filter (AOTF) can select optical wavelengths at a very high speed and with a high resolution, depending on the driving system, as well as the used AO material.

Other possible AO devices usable in space applications are AO Deflectors (AODs), Modulators (AOMs) and Frequency Shifters (AOFSs). Each device has its specific optical behavior.

The AOD can be used as a spatial light modulator for encoding electrical info onto an optical beam [4], or as a device in the multichannel transmission of optical information [5]. The latter has the advantage of splitting the incoming light beam into several independently controlled beams without substantial loss of light-power.

The AOM can be used for the generation of phase-locked laser light [6]. This device can also be applied in laser satellite communication, which makes use of the travelling grating mode feature of AOMs [7]. In laser satellite communications, an AOFS can be used in the same way as an AOM.

Additionally, the AOFS can be utilized to delay an optical signal applied in a fiber [8]. This can be used to investigate the behavior of a cavity semiconductor laser, by applying the delayed self-heterodyne interferometric technique [9].

The main advantage of these AO devices is the ability to work in the harsh environment of space, without using an active mechanism. Most applications where a selection, modulation, shifting or deflection of an optical light beam is necessary still rely on moving mechanisms. Avoiding moving mechanical parts is a key driver for future miniaturization, as well as improvements in robustness and reliability. Hence, many different applications are possible in using these devices.

All these AO devices are activated by a Radio Frequency (RF) signal. This necessitates an RF signal generator which can survive the harsh environment of space. This driving system generates an RF signal of a certain frequency and power level, which is applied to a transducer of the AO device. This transducer is responsible for the conversion of the RF signal into sound waves. The transducer is mounted to the side of the AO crystal and contains a piezoelectric element which is responsible for the RF to sound wave conversion. These sound waves propagate through the AO material and interact with the incoming light beam, resulting in the desired effect.

2. AO materials and principles

In general, AO devices make use of different kind of materials as an optical element [10, 4]. Each material has a specific optical wavelength domain in which they can be used. The way these materials must be driven also differs.

Table 1. Examples of used AO material and the applicable transparency window.

Material	*Transparency window [μm]*
Quartz (SiO_2)	$0.18 - 3.5$
KDP (KH_2PO_4)	$0.21 - 1.5$
TeO_2	$0.35 - 5.0$
Hg_2Cl_2	$0.38 - 28$
Hg_2Br_2	$0.4 - 30$
Te	$4 - 20$
$LiNbO_3$	$0.4 - 4.5$

For applications in specific optical wavelength domains, e.g. the near-, far- and mid-infrared region, new materials such as Ge–Se–Te alloys are being developed [11]. In AOTF space applications the selection is generally limited to tellurium dioxide (TeO_2) and quartz (SiO_2) [12], although more exotic materials like potassium dihydrogen phosphate (KDP) are being researched.

A piezoelectric transducer glued to this AO material converts an applied RF signal into sound waves which propagate inside this AO material. These sound waves interact with the incoming light beam and, due to the principle of birefringence, several output beams are created. The light beam applied at the entrance of the AO device undergoes Bragg diffraction, as illustrated in figure 1. The Bragg regime is used for AOMs, AOFSs, AOTFs and AODs. For this to work, the applied light beam must fulfill the Bragg condition [4]:

$$\sin\theta_B = \frac{\lambda}{2\Delta} \tag{1}$$

In which θ_B is defined as the Bragg angle, λ the wavelength of the light entering the AO device and Δ the acoustic wavelength inside the AO material.

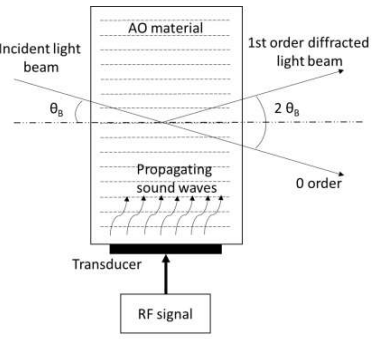

Figure 1. Light entering according to the Bragg regime.

3. Flexible RF generator for AO devices

As shown in figure 2, the general driving system for AO devices consist of two parts: 1) a uniform RF generator and 2) an RF amplifier. The RF generator generates a sine wave at a target frequency. The power level of this signal is limited to around 0 dBm, so an RF amplifier is connected in series with the generator. The amplifier increases the power level to around +30 dBm. The exact power level is varied according to the material of the AO device in question.

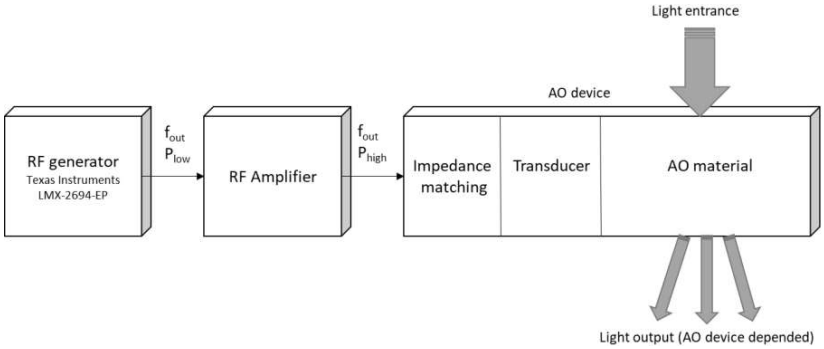

Figure 2. RF driving chain for AO devices.

The RF-to-acoustic transducer is coupled to the AO device through an impedance matching network. Depending on the used AO device (AOTF, AOM, AOFS or AOD), the way light exits the AO device varies.

This research focuses on the design of the first component, and aims at having a flexible, uniform RF generator suitable for driving multiple AO devices (AOTF, AOM, AOFS and AOD). This RF generator must satisfy a number of practical design requirements, based on general scientific requirements for AO devices. These practical key parameters are listed in table 2.

Table 2. Key requirements of the uniform RF generator.

Requirement	*Value*	*Unit*
Output power	> 0	dBm
Harmonic and spur suppression	< -30	dBc
Frequency range	40 – 300	MHz
Resolution	< 1	kHz
Power consumption	< 2	W
Output impedance	50	Ohm

For several applications, the RF signal applied to the transducer should be a pure sinewave. In case other RF signals enter the transducer, the optical behavior of the AO device will be distorted. Hence, the suppression of harmonics and spurs needs to be below 30 dB compared to the carrier signal.

The frequency range at the output of the RF generator is set at 40 to 300 MHz. This should cover the frequency range for the space applications in which AO devices are envisaged in this paper.

In order to select the appropriate spectral line in an accurate way, the RF output signal needs to have a resolution of 1 kHz.

The power consumption should preferably be below 2 W, especially in the frame of space applications.

As the RF generator is connected to an RF amplifier as illustrated in figure 2, both devices should have a 50 Ohm load impedance.

3.1. Design setup of a uniform RF generator

All AO devices work with an RF signal applied to the transducer. The generation of this signal must be done using specific space qualified components in order to withstand the harsh operating environment of space. The availability of these kind of components is rather limited. In case the RF generator is used for scientific missions for Agencies such as ESA or NASA, specific requirements come into play, i.e. the European Cooperation for Space Standardization (ECSS) regulation. For commercial missions, greater component selection flexibility is available. Still, the components used must withstand intense radiation, thermal cycling and shock, depending on the objectives of the (deep) space mission.

In this design, a commercial-off-the-shelf space qualified Phase-Locked Loop (PLL) chip, combined with a power section, a microcontroller, electronically switched filter banks, and supporting components are used as shown in figure 3.

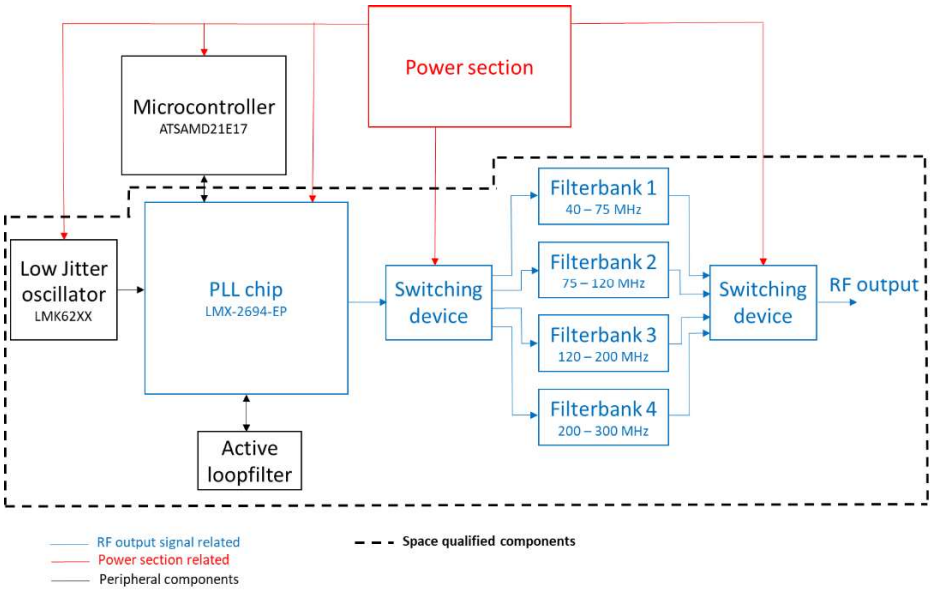

Figure 3. RF generator setup.

The commercially available space qualified PLL LMX-2694-EP chip of Texas Instrument [13] is the key component of the signal generator. The chip can generate an output signal in a broad frequency range from 39.3 MHz to 15.1 GHz, and runs on a single power supply of +3.3 V. In order to cover this wide frequency range, the chip uses several selectable internal Voltage Controlled Oscillators (VCOs) which operate between 8.1 GHz and 14.7 GHz. By using internal dividers, the frequency is downscaled. A fractional N-PLL with a delta-sigma modulator is used. Hence, very small frequency steps down to 1

Hz can be obtained. This fits the 1 kHz resolution requirement. Additionally, the needed RF output frequency range fits the requested 40 to 300 MHz. If higher frequencies (GHz-range) for other or future space applications are needed, this can also be fulfilled.

This device has an identical radiation hardened counterpart, the LMX-2694-SEP [14]. The functionality of both chips is exactly the same. Hence, a one-to-one transition from the engineering design (EP-version) into a space qualified design (SEP-version) is possible. The test results will also be comparable.

In order to drive the LMX-2694-EP, a dedicated microcontroller is necessary. For space applications several microcontrollers exist. Depending on the future integration of the RF generator, this task can also be carried out by a centrally implemented Field-Programmable Gate Array (FPGA) or another device. Hence, for the design at this level, a general-purpose microcontroller is used for activating the LMX-2694-EP and the necessary filter banks. This reasoning is also valid for the power section. The different devices can be powered using the satellite power bus aboard the spacecraft. If not, dedicated linear and switching regulators exist in a space qualified package [15]. All components, including the PLL, RF switching devices and oscillator, run on a single power supply of +3.3 V, which simplifies the power section design.

In figure 3, all components which should be selected keeping a space qualification in mind, are delineated with a dash-dotted box. The in-house designed electronically switched filter banks are made of passive components. These filter banks are connected to the RF output connector and the LMX-2694-EP using two switching devices. In this design, two MiniCircuits HSWA4-63DR+ SP4T Monolithic Microwave Integrated Circuit (MMIC) switches are used [16]. This part can be up screened into a space qualified component by MiniCircuits. Other space qualified switches are also available on the market, like the ADH244S from Analog Devices [15]. The PLL chip needs a reference oscillator signal. This is generated by the LMK62XX from Texas Instruments [17]. The latter can be replaced with a space qualified component from Vectron [18] if necessary. The active loop filter consists of passive resistors and capacitors, which are widely available in space qualified packaging.

3.2. Measurement results of the PLL chip

The LMX-2694-EP was tested as a standalone device, using the LMX2694EPEVM evaluation board version of the chip [13]. Several aspects were checked, such as the RF output spectrum and resolution, the generated harmonics (2^{nd} and 3^{rd}), the generated output power level of the chip, as well as the power consumption.

In figure 4 the RF output spectrum generated by the LMX-2694 is shown. The frequency range from 40 MHz to 300 MHz was easily reached, together with the resolution of 1 kHz. The RF output spectrum contains multiple harmonics and spurs which need to be removed by the filter banks.

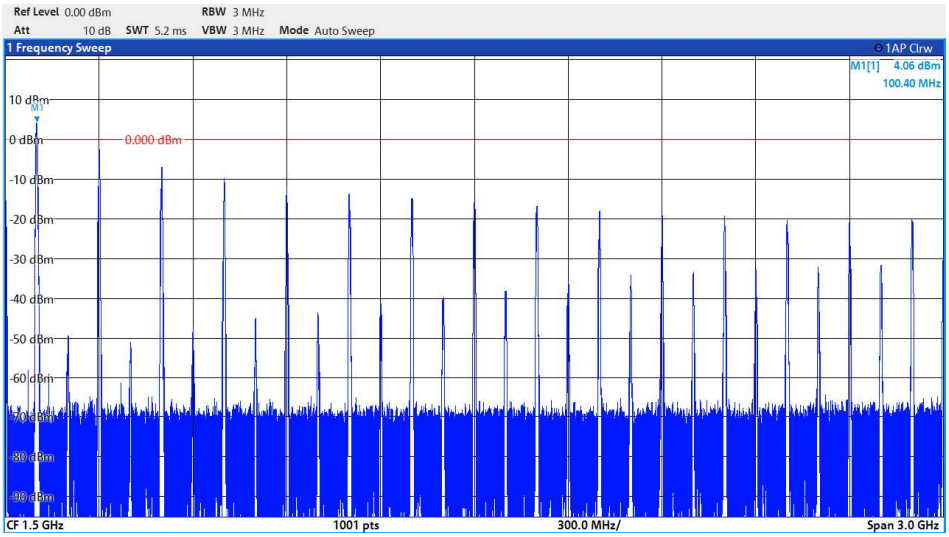

Figure 4. The RF output spectrum at 100 MHz.

In figure 5 the levels of the second and third harmonics are shown in the frequency range applicable for AO devices. Especially the third harmonic needs additional suppression to be below -30 dBc.

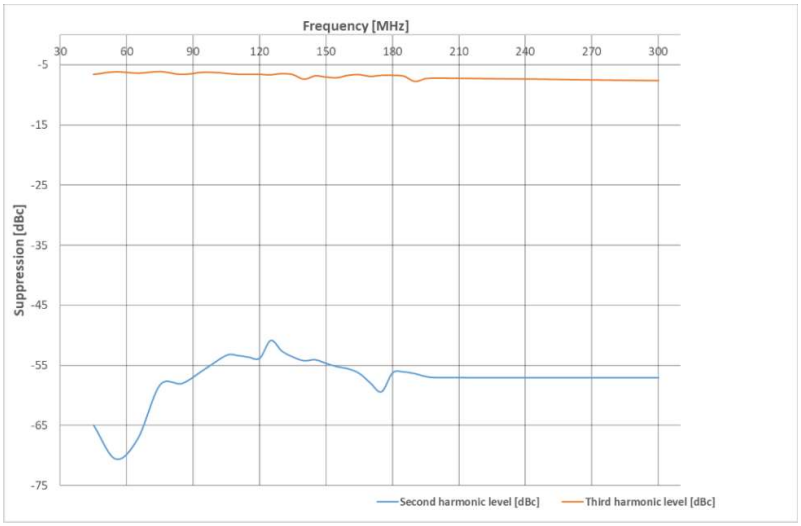

Figure 5. Second and third harmonic level at different RF output frequencies.

The output power level of the chip can be programmed and depends on the requested RF output frequency. Depending on the internal value setting of the chip, the RF output power level varies between 2.2 and 5 dBm. Keep in mind that the final output power level will be lower due to losses in the passive filter banks and switching devices.

The power consumption depends on the internal settings, but the measured value in a single output operation mode is around 1.1 W.

3.3. Simulation results of the different filter banks

The filter banks need to provide the necessary attenuation of spurs and harmonics generated by the PLL chip. The third harmonic has a particularly high amplitude and needs sufficient suppression to be below

-30 dBc. This requires sufficiently steep roll-off past the filter cutoff frequency, which largely drove filter selection and design. The amplitude of the second harmonic is limited and more easily suppressed.

The filter banks cover four frequency ranges, each limited to less than one octave. This prevents overlap between the second harmonic of the lowest frequency setting, and the fundamental of the highest frequency setting. The four ranges are: 40 MHz to 75 MHz, 75 MHz to 120 MHz, 120 MHz to 200 MHz and 200 MHz to 300 MHz. The general electrical circuit design for the filters is shown in figure 6. It is a fifth-order Chebyshev filter, and only contains passive components. An example of the 40-75 MHz filter curve is presented in figure 7.

By switching between these different banks, the full frequency range from 40 MHz up to 300 MHz can be covered. The cut off performance of the filter curves are in line with the -30 dBc requirement. The combination of the PLL chip, switching devices and the filter banks should result in an output power level around 0 dBm.

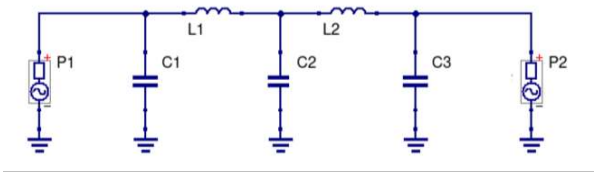

Figure 6. Design of the filter bank.

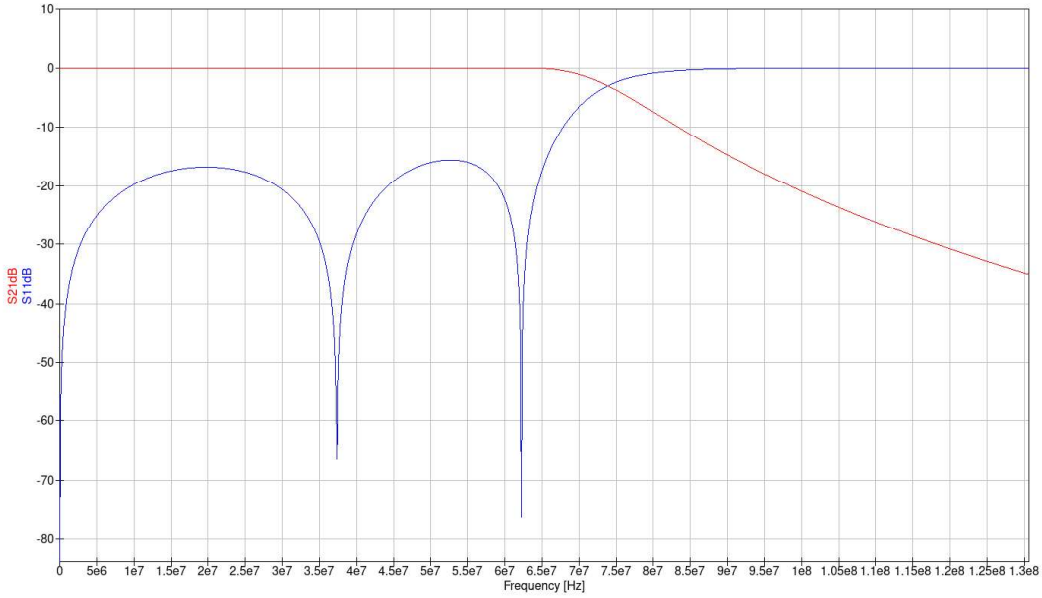

Figure 7. Simulation results of the 40-75 MHz filter bank.

4. Conclusion and future work

This report presented the key considerations and preliminary design work of an RF generator able to steer various AO devices. A commercial-off-the-shelf PLL chip from Texas Instruments was also characterized as a stand-alone device. All key requirements necessary for the RF generator were examined. Preliminary results show that the LMX-2694-EP is suitable for driving AO devices in multiple future space applications. Further suppression of the harmonics, especially the third harmonic, was necessary. Hence, a dedicated filter bank was developed. These separate filters, all limited to less than one octave, were simulated and showed good results in line with their requirements.

The next step will be building and testing the integrated PLL board, the filter banks and all supporting electronics. This design can then be transformed into a fully space qualified RF generator.

References

[1] J.R. Kerr, P.J. Titterton, A.R. Kraemer and C.R. Cooke 1970 Atmospheric Optical Communications Systems *Proceedings of the IEEE* **58** 10 pp 1691-1709
[2] E. Swanson and V. Chan 1986 Heterodyne Spatial Tracking System for Optical Space Communication *IEEE Transactions on Communications* **34** 2 pp 118-126
[3] S. Robert et al. 2016 Expected Performances of the NOMAD/ExoMars Instrument *Planetary and Space Science* **124** pp 94–104
[4] A.P. Goutzoulis and D.R. Pape 1994 *Design and Fabrication of Acousto-Optic Devices* New York-Basel-Hong Kong Marcel Dekker Inc.
[5] S.N. Antonov and Yu.G. Rezvov 2020 Acousto-Optic Devices Based on Multibeam Diffraction *Instrum Exp Tech* **63** pp 835–841
[6] F.B.J. Buchkremer, R. Dumke, Ch. Buggle, G. Brikl and W. Ertmer 2000 Low-Cost Setup for Generation of 3 GHz Frequency Difference Phase-Locked Laser Light *Review of Scientific Instruments* **71** 9 pp 3306–3308
[7] E. Fischer, P. Adolph, T. Weigel, C. Haupt and G. Baister 2001 Advanced optical solutions for inter-satellite communications *Optik* **112** 9 pp 442–448
[8] Z. Xia, W. Xie, D. Sun, H. Shi, Y. Dong and W. Hu 2013 Photonic Generation of Linearly Chirped Millimeter Wave Based on Comb-Spacing Tunable Optical Frequency Comb *Optical Engineering* **52** 12 pp 126107-1 – 5
[9] L. Richter, H. Mandelberg, M. Kruger and P. McGrath 1986 Linewidth Determination from Self-Heterodyne Measurements with Subcoherence Delay Times *IEEE Journal of Quantum Electronics* **22** 11 pp 2070–2074
[10] J.S. Kim, S.B. Trivedi, J. Soos, N. Gupta and W. Palosz 2007 Development of mercurous halide crystals for acousto-optic devices *Proceedings SPIE, Imaging Spectrometry XII* **6661** 1 (San Diego, California, USA) pp 66610B – 66610B-12
[11] L.A. Kulakova, B.T. Melekh, S.A. Grudinkin and A.P. Danilov 2013 Ge-Te-Se and Ge-Te-Se-S Alloys as New Materials for Acousto-Optic Devices of the near-, Mid-, and Far-Infrared Spectral Regions *Semiconductors (Woodbury, N.Y.)* **47** 10 pp 1426–1431
[12] O. I. Korablev, D. A. Belyaev, Y.S. Dobrolenskiy, A.Y. Trokhimovskiy and Y.K. Kalinnikov 2018 Acousto-optic tunable filter spectrometers in space missions [Invited] *Appl. Opt.* **57** 10 pp C103-C119
[13] LMX-2694-EP chip, Texas Instruments, Datasheet, https://www.ti.com/product/LMX2694-EP [online], accessed on 12th July 2022
[14] LMX-2684-SEP chip, Texas Instruments, Datasheet, https://www.ti.com/product/LMX2694-SEP [online], accessed on the 12th of July 2022
[15] Analog Devices, Space Qualified Parts List, https://www.analog.com/media/en/news-marketing-collateral/product-selection-guide/SpaceQualifiedPartsList.pdf [online], accessed on the 20th July 2022
[16] HSWA4-63DR+ SP4T RF Switch, MiniCircuits, Datasheet, https://www.minicircuits.com/pdfs/HSWA4-63DR+.pdf [online], accessed on the 20th of July 2022
[17] LMK62XX, Texas Instruments, Datasheet, https://www.ti.com/lit/ds/symlink/lmk62a2-156m.pdf?ts=1658320419295&ref_url=https%253A%252F%252Fwww.google.be%252F [online], accessed on the 20th of July 2022
[18] Vectron, "Space and Hi-rel products", Datasheet, https://www.vectron.com/products/space/space.htm, [online], accessed on the 26th of August 2022